CrossMark

Hot Workability and Superplasticity of Low-Al and High-Nb Containing TiAl Alloys

BIN TANG,[1,2,3] FENGTONG ZHAO,[1] YUDONG CHU,[1] HONGCHAO KOU,[1,2] and JINSHAN LI[1,2]

1.—State Key Laboratory of Solidification Processing, Northwestern Polytechnical University, No. 127, Youyi Xilu, Xi'an 710072, Shaanxi, People's Republic of China. 2.—National & Local Joint Engineering Research Center for Precision Thermal Forming Technology of Advanced Metal Materials, Northwestern Polytechnical University, Xi'an 710072, Shaanxi, People's Republic of China. 3.—e-mail: toby198489@163.com

The superplastic deformation mechanism of low-Al and high-Nb containing TiAl alloy was investigated in compression mode. The experimental results showed that intense dynamic recrystallization (DRX) breaks the balance and leads to a significant drop in flow stress after the peak when deforming below 950°C. Arrhenius kinetic analysis revealed that the activation energy for superplastic compression first increased then decreased with temperature, suggesting a change in the deformation mechanism. Microstructure observations showed that, when deformed at 850°C, the deformation mechanism was grain-boundary sliding accommodated by γ-DRX, γ-intragranular deformation, and β/B2-phase decomposition, while the mechanism was grain-boundary sliding accommodated by γ-DRX, β/B2-DRX, and $\gamma \rightarrow \beta$/B2 + α_2 phase transformation when deformed at 1000°C. After compression, the microstructure tended to be uniform, which may yield important information for the development of new deformation techniques for TiAl alloys.

INTRODUCTION

TiAl alloys are considered to be some of the most important candidates to replace Ni-based superalloys and high-temperature titanium alloys for use in aero-engines.[1,2] However, the applications of TiAl alloys are limited by their intrinsic brittleness and hard workability. Recently, a new class of TiAl-based alloys, named β–γ TiAl alloys, has been developed for engineering applications, exhibiting excellent hot deformability.[3,4] According to Kim Ref. 3 the composition range of β–γ TiAl alloys is Ti-(40–45)Al-(2–8)Nb-(1–8)(Mn, Cr, Mo, V)-(0.2–0.6) (B, C). β–γ TiAl alloys that solidify via the β-phase can be manufactured using conventional hot forging operations and equipment.[5–7] Moreover, a larger amount of β/B2-phase will be preserved during the cooling process as a result of nonequilibrium solidification, improving the deformability of such TiAl alloys at high temperature.[8] As typical β–γ TiAl alloys, low-Al and high-Nb containing TiAl alloys with (β/B2 + γ) microstructure have been found to exhibit superplastic deformation in the temperature range from 850°C to 1050°C at strain rate of 10^{-4} s^{-1}.[9,10] Based on this superplastic property, TiAl alloys have potential to form complex structures, favoring their industry application. However, the superplasticity of such low-Al and high-Nb containing TiAl alloys has not been studied in compression mode. Besides, the superplastic deformation mechanism is predicted to be complex, as the deformation process may be accompanied by decomposition of β/B2-phase[11] or other phase transformations.

The aim of the present work is to provide fundamental understanding of the superplastic compression mechanism for low-Al and high-Nb containing TiAl alloys. Based on the Arrhenius stress constitutive equation, the changes of the deformation activation energy and stress exponent with compression temperature were analyzed. Using the electron backscatter diffraction (EBSD) technique, the dynamic recrystallization (DRX) behavior and phase transformation are discussed. These results ultimately contribute to
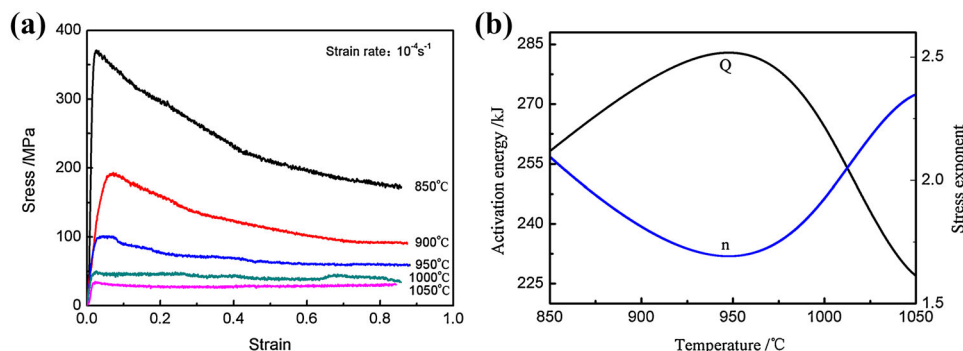
Fig. 1. (a) Flow stress–strain curves of Ti-42.5Al-8Nb-0.2W-0.2B-0.1Y alloy isothermally compressed at different temperatures at strain rate of 10^{-4} s^{-1} and (b) the values of Q and n as functions of temperature.

understanding of the superplastic deformation behavior, favoring development of new forming technologies for TiAl alloys.

MATERIALS AND EXPERIMENTAL PROCEDURES

A TiAl ingot with composition Ti-42.5Al-8Nb-0.2W-0.2B-0.1Y was prepared by the triple vacuum arc remelting (VAR) method. The ingot was subjected to hot isostatic pressing at 1300°C for 4 h under pressure of 140 MPa and subsequently hot-forged at 1260°C. Compression samples (Φ = 8 mm, aspect ratio 1.5:1) with a 0.1-mm-deep ring groove at the ends were machined from the forged pancake; the compression direction was parallel to the forging direction.

Thermal simulation compression tests were carried out on the cylindrical simples using a Fuji radio Thermemcmastor-Z thermo mechanical simulator at deformation temperature of 850, 900, 950, 1000, and 1050°C at constant strain rate of 10^{-4} s^{-1}. Before deformation, the annular groove at the end of the cylindrical sample was filled with glass powder lubricant to reduce friction during the loading process. Besides, a mica sheet was placed between the sample ends and silicon nitride anvil. All the samples were heated using an induction heating system at rate of 10 K/s from room temperature to the test temperature and kept at that temperature for 5 min to ensure a uniform temperature distribution throughout the sample. All hot compression tests were carried out in vacuum environment. Samples were compressed to 60% reduction in height, then quenched using helium at cooling rate of 50 K/s to freeze the microstructure.

After deformation, the samples were cut along the compression axis by electron discharge machining for microstructural analysis. The microstructure was mainly characterized by high-resolution field-emission scanning electron microscopy (FESEM) equipped with an EBSD system operating at 20 kV. EBSD samples were prepared by conventional metallographic methods followed by vibration polishing in a VIBROET2 vibration polishing machine for 7 h to produce a surface free of, or with little, residual stress. EBSD measurements were carried out with scan step size of 0.2 μm on a rectangular scan grid.

RESULTS AND DISCUSSION

Kinetic Analysis of the Isothermal Compression Process

Figure 1a shows the flow curves obtained during the isothermal compression process of the alloy at deformation temperature of 850–1050°C and strain rate of 10^{-4} s^{-1}. As shown in Fig. 1a, the flow stress presented significant softening behavior after the peak when compressing at 850°C. On increasing the temperature to 900°C or 950°C, the softening rate decreased obviously. For the samples compressed at 1000°C and 1050°C, the flow stress reached steady-state directly after the peak stress. A similar softening tendency was found during the deformation process of TA15 titanium alloy[12] and Ti-22Al-25Nb alloy.[13] DRX is considered to play an important role in the rapid drop of flow stress, and the detailed mechanism is discussed in the next section.

According to the flow stress curves, the constitutive relationship between the flow stress (σ), strain rate ($\dot{\varepsilon}$), and deformation temperature (T) during the compression process can be expressed using the following Arrhenius-type equation:[14]

$$\dot{\varepsilon} = A \cdot \exp\left(-\frac{Q}{RT}\right) \cdot \left(\frac{\sigma}{E}\right)^n, \qquad (1)$$

where Q is the activation energy correlated with the deformation mechanism, E is the Young's modulus, R is the universal gas constant, and A is a material constant. To clarify the kinetic characteristics of the present alloy during the superplastic compression process, the parameters (Q and n) in this constitutive equation were derived from the test data shown in Fig. 1a by using the peak stress values.

According to Eq. 1, the relationship between Q and n can be obtained as

$$Q = n \times R \times \partial \ln\left(\frac{\sigma}{E}\right) \Big/ \partial\left(\frac{1}{T}\right), \qquad (2)$$

$$n = (\ln \dot{\varepsilon} - \ln A) \Big/ \left\{ \ln\left(\frac{\sigma}{E}\right) - \frac{1}{T}\left[\partial \ln\left(\frac{\sigma}{E}\right) \Big/ \partial\left(\frac{1}{T}\right)\right]\right\}. \qquad (3)$$

To derive the solution, one first needs to calculate the value of ln A, because the parameters $\dot{\varepsilon}$, E, σ, and T are known for the present condition. Therefore, an additional compression experiment (at 1000°C and 10^{-5} s^{-1}) was carried out to calculate the value of n at 1000°C. The obtained peak stress was about 12.5 MPa. Then, the value of n at 1000°C can be calculated using the classical equation.[15]

$$n = \frac{\partial \ln \dot{\varepsilon}}{\partial \ln \sigma} = \left(\ln \frac{\dot{\varepsilon}_2}{\dot{\varepsilon}_1}\right) \Big/ \left(\ln \frac{\sigma_2}{\sigma_1}\right). \qquad (4)$$

Using this equation, the value of n at 1000°C was calculated to be ~2. Using Eq. 3, the value of ln A can then be obtained. Then, the values of Q and n at different temperatures were calculated using Eqs. 2 and 3. To reduce the error, the peak stress values at different temperatures in steps of 1°C were calculated using interpolation before calculating the value of n. The values of Q and n versus deformation temperature for the present alloy are illustrated in Fig. 1b. As shown in Fig. 1b, the stress exponent changed between 1.71 and 2.35 (~2), indicating a superplastic deformation process. Moreover, the predominant deformation mechanism was grain-boundary sliding. Besides, the activation energy for superplastic compression was found first to increase then to decrease with temperature. This indicates that the rate-controlling mechanism changed with increase of the deformation temperature. We also found that the activation energy was smaller than the self-diffusion energy of Al atoms in the γ-TiAl lattice[16] but larger than the self-diffusion activation energy of β-Ti.[17] This implies that the deformation mechanism may be controlled by a mixed mechanism of γ-lattice diffusion and β-lattice diffusion. It also suggests that the controlling mechanism for the alloy with ($\gamma + \beta$/B2) microstructure is different from that of the same alloy but with ($\gamma + \alpha_2$) microstructure.[18]

Deformation Mechanism During Superplastic Compression

Figure 2 shows the initial microstructure of the Ti-42.5Al-8Nb-0.2W-0.2B-0.1Y alloy. The EBSD image shows that the initial microstructure mainly consisted of equiaxial γ-grains and β/B2-phase. Meanwhile, a little α_2-phase is also observed in the matrix. The γ-phase in the microstructure can be classified into two types: relatively coarse grains with average size of 10 μm and fine grains with
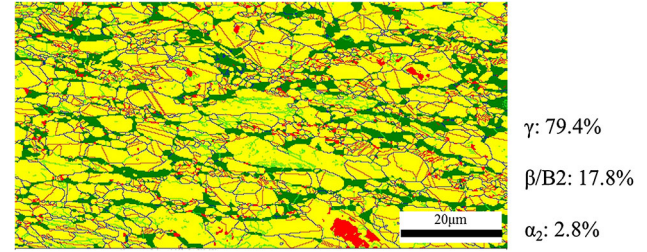

γ: 79.4%

β/B2: 17.8%

α₂: 2.8%

Fig. 2. Phase map with grain and twin boundaries of Ti-42.5Al-8Nb-0.2W-0.2B-0.1Y alloy at initial state (γ-phase in yellow, B2 in green, α_2 in red) (Color figure online).

average size of 4 μm. The fine γ-grains are considered to be produced through β/B2 → γ phase transformation during the cooling process. The volume fractions of γ-, β/B2-, and α_2-phase were about 79.4%, 17.8%, and 2.8%, respectively. Our previous studies showed that a large amount of β/B2-phase was obtained by forging in the ($\alpha + \beta$)-phase region,[7] favoring hot deformation of TiAl alloys. Besides, the type of grain boundary is also shown in the EBSD image, with blue lines representing high-angle grain boundaries (HAGBs) with misorientation (θ) greater than 15° and black lines representing low-angle grain boundaries (LAGBs) with 2° < θ < 15°. Specifically, grain boundaries with 59° < θ < 61° are thought to be twin boundaries (TB), represented by red lines. In Fig. 2, the fractions of HAGBs, LAGBs, and TBs are about 44%, 25%, and 31%, respectively.

It can be seen from Fig. 1b that the Q–T curve first increases then decreases, which may correspond to two kinds of controlling mechanism. Therefore, the samples compressed at 850°C, 900°C, and 1000°C were chosen for EBSD analysis. Figure 3 shows the microstructure in the center part of samples compressed at different temperatures. As shown in Fig. 3a, numerous γ recrystallization grains with extra fine size were found after compressing at 850°C. This may be the reason for the obvious drop in flow stress after the peak in Fig. 1a. The intense occurrence of DRX has the ability to break the balance between dislocation hardening and dynamic recovery and thus preclude constant flow stress. When the temperature was increased to 900°C, the γ recrystallization grains increased significantly (Fig. 3b). On further increase of the deformation temperature to 1000°C, the size of the γ recrystallization grains continued to increase (Fig. 3c). Figure 4a shows the size distribution of γ-grains for different deformation conditions. As shown in Fig. 4a, the fraction of extra fine grains markedly decreased with increase of the deformation temperature, and the microstructure of the alloy tended to become more uniform. Besides, we also found that the volume fraction of β/B2-phase decreased when compressing at 850°C, while the volume fraction of β/B2-phase and α_2-phase obviously increased when compressing at 1000°C. Furthermore, as shown in
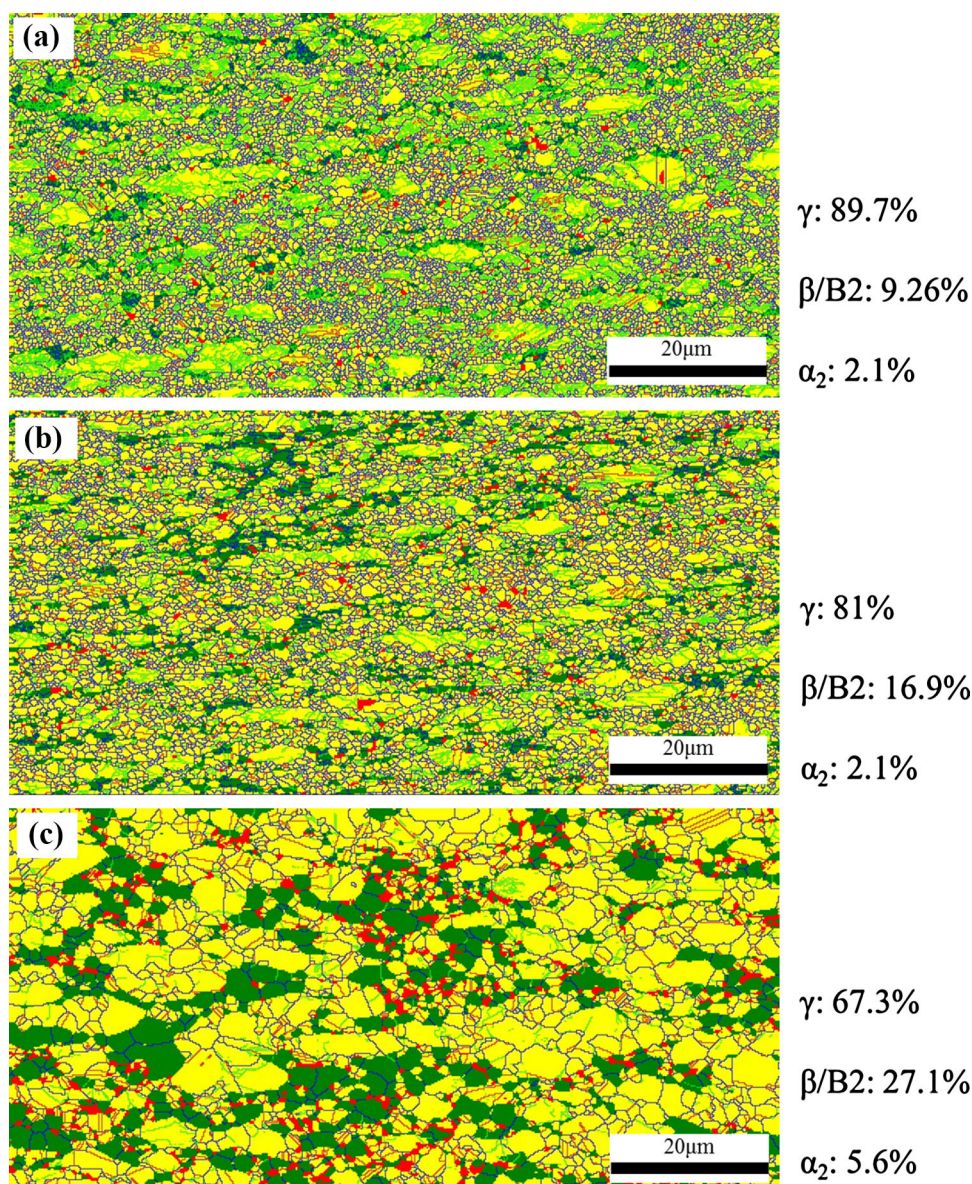
Fig. 3. Phase map with grain and twin boundaries of Ti-42.5Al-8Nb-0.2W-0.2B-0.1Y alloy compressed at (a) 850°C, (b) 900°C, and (c) 1000°C (γ-phase in yellow, B2 in green, α_2 in red) (Color figure online).

Fig. 3c, the α_2-phase was found to always appear with β/B2-phase. This suggests that the $\gamma \rightarrow \beta$/B2 + α_2 phase transformation occurred when compressing at 1000°C, while the β/B2-phase tended to decompose when compressing at 850°C. Therefore, one can suggest that the $\gamma \rightarrow \beta$/B2 + α_2 phase transformation plays an important role in the decrease of the Q value after 950°C, as the β/B2-phase is a soft phase at high temperature, favoring superplastic deformation.

Furthermore, the change in the misorientation of the grain boundaries with increase of the deformation temperature was investigated to explore the controlling mechanism of the superplastic compression process. As shown in Fig. 4b, the number fraction of HAGBs increased from 44 to 60, 68,

and 62 when the deformation temperature was increased from 850°C to 1000°C, respectively. Note that grain-boundary sliding plays an important role in the superplastic deformation process.[19] Meanwhile, the number fraction of LAGBs increased from 25% to 35% when compressing at 850°C, but then decreased to 23% and 16% when compressing at 900°C and 1000°C, respectively. This indicates that intense intragranular deformation occurred at 850°C. Besides, the number fraction of TBs decreased obviously after compressing at 850°C (from 31% to 5%) and 900°C (from 31% to 9%), while the change was relatively slightly after compressing at 1000°C (from 31% to 22%). Note that the twinning-related γ-phase DRX nucleation mechanism plays an important role in the compression
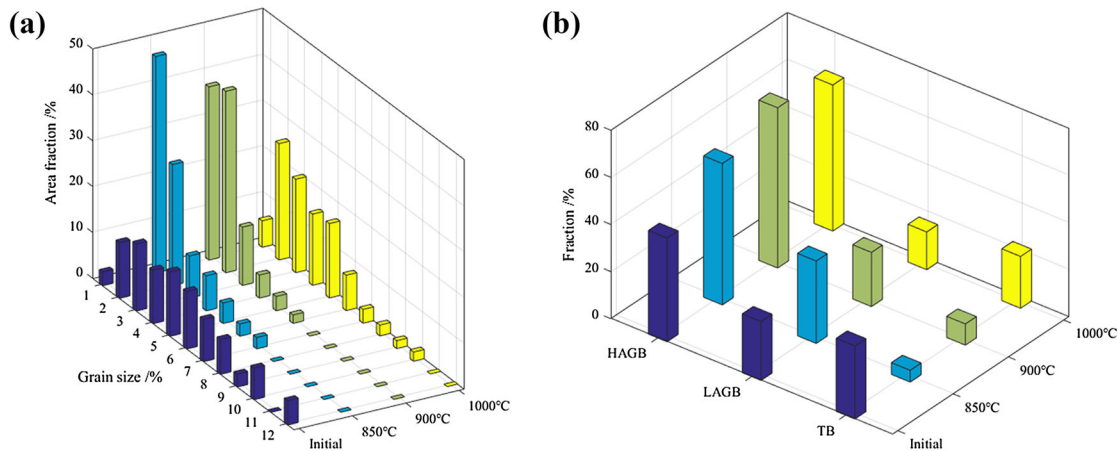
Fig. 4. Distribution of (a) γ grain size and (b) HAGBs, LAGBs, and TBs at different deformation temperatures.

process at 850°C and 900°C. Except for the study of misorientation of γ-grain boundaries, we also found that many HAGBs appeared in β/B2-phase (from Fig. 3c), providing clear evidence of the occurrence of β/B2-phase DRX. This seems to be contradictory to the general consensus regarding the action of β/B2-phase in TiAl alloys, which is considered to undergo plastic deformation during the hot-working process due to its soft nature.[20]

CONCLUSION

The superplastic compression behavior of a low-Al and high-Nb containing TiAl alloy with nominal composition Ti-42.5Al-8Nb-0.2W-0.2B-0.1Y was investigated. Based on Arrhenius kinetic analysis, the change of the activation energy with deformation temperature was discussed. EBSD observations were used to detect the evolution of grain boundaries, DRX, and phase transformation. The deformation mechanism during the superplastic compression process was proposed. The main results can be summarized as follows:

1. The alloy exhibited superplastic deformation ability in compression mode in the temperature range from 850°C to 1000°C and strain rate of 10^{-4} s^{-1}. Meanwhile, the activation energy for superplastic compression was found to first increase then decrease with deformation temperature.
2. For compression at 850°C, the superplastic deformation mechanism was grain-boundary sliding accommodated by γ-phase DRX, γ intragranular deformation, and β/B2-phase decomposition.
3. For compression at 1000°C, the superplastic deformation mechanism was grain-boundary sliding accommodated by γ-phase DRX, β/B2-phase DRX, and $\gamma \rightarrow \beta$/B2 + α_2 phase transformation. After compression, the volume fraction of β/B2-phase and α_2 increased and the microstructure tended to become more uniform.

REFERENCES

1. D.M. Dimiduk, *Mater. Sci. Eng. A* 263, 281 (1999).
2. P. Janschek, *Mater. Today* 2S, S92 (2015).
3. D.S. Shih and Y.W. Kim, *Ti-2007 Science and Technology*, ed. M. Ninomi (Sendai: The Japan Institute of Metals, 2007), pp. 1021–1024.
4. J.S. Kim, Y.H. Lee, Y.W. Kim, and C.S. Lee, *Mater. Sci. Forum* 539–543, 1531 (2007).
5. T. Tetsui, K. Shindo, S. Kaji, S. Kobayashi, and M. Takeyama, *Intermetallics* 13, 971 (2005).
6. T. Tetsui, K. Shindo, S. Kobayashi, and M. Takeyama, *Intermetallics* 11, 299 (2003).
7. B. Tang, L. Cheng, H.C. Kou, and J.S. Li, *Intermetallics* 58, 7 (2015).
8. B. Tang, W.C. Ou, H.C. Kou, and J.S. Li, *Mater. Charact.* 109, 122 (2015).
9. L. Cheng, Y. Chen, J.S. Li, and E. Bouzy, *Mater. Lett.* 194, 58 (2017).
10. L. Cheng, J.S. Li, X.Y. Xue, B. Tang, H.C. Kou, O. Perroud, and E. Bouzy, *J. Alloys Compd.* 693, 749 (2017).
11. D. Zhang, G. Dehm, and H. Clemens, *Scr. Mater.* 42, 1065 (2000).
12. P.F. Gao, M. Zhan, X.G. Fan, Z.N. Lei, and Y. Cai, *Mater. Sci. Eng. A* 689, 243 (2017).
13. X. Ma, W.D. Zeng, B. Xu, Y. Sun, C. Xue, and Y.F. Han, *Intermetallics* 20, 1 (2012).
14. Y.V.R.K. Prasad and T. Seshacharyulu, *Int. Mater. Rev.* 43, 243 (1998).
15. M.E. Kassner and M.T. Perez-Prado, *Prog. Mater. Sci.* 45, 1 (2000).
16. Y. Mishin and C. Herzig, *Acta Mater.* 48, 589 (2000).
17. P.M. Sargent and M.F. Ashby, *Scr. Metall. Mater.* 16, 1415 (1982).
18. L. Cheng, J.S. Li, X.Y. Xue, B. Tang, H.C. Kou, and E. Bouzy, *Intermetallics* 75, 62 (2016).
19. Z.X. Du, J.S. Liu, G.W. Li, K. Lv, G.L. Liu, L.M. Yan, and Y.Y. Chen, *Mater. Sci. Eng. A* 650, 414 (2016).
20. F. Appel, H. Clemens, and F.D. Fischer, *Prog. Mater. Sci.* 81, 55 (2016).